P. DRZYMAŁA*, B. KANIA*, M. WRÓBEL**, P. DARŁAK***, P. DŁUGOSZ***, P. KWAŚNIEWSKI**, J. T. BONARSKI*

EVOLUTION OF MICROSTRUCTURE IN ROLLED Mg-BASED ALLOY. TEXTURAL ASPECT

EWOLUCJA MIKROSTRUKTURY W WALCOWANYM STOPIE NA BAZIE Mg. ASPEKT TEKSTUROWY

Magnesium alloys are the lightest structural materials, which makes them particularly suitable for use in the aircraft and automotive industry. However, due to hexagonal close-packed crystal structure, resulting in insufficient number of independent slip systems, magnesium alloys exhibit poor formability at room temperature. Conventional methods of work hardening of magnesium alloys requires the temperature about 300°C, which favours simultaneously processes of thermal recovery and grain growth, but decreases beneficial microstructure strengthening effect. Thus, it is a crucial to undertake development of a technology for semi-finished magnesium alloys elements, which will ensure better mechanical properties of the final products by forming desirable microstructure. In the paper we present the development of crystallographic texture of the Mg-based alloy (Mg-AZ31) in the form of pipe extruded at 430°C and subjected to pilger rolling at relatively low temperature.

Keywords: magnesium alloy, plastic deformation, pilger rolling, mechanical twinning, crystallographic texture

Stopy magnezu należą do najlżejszych materiałów konstrukcyjnych, co czyni je szczególnie użytecznymi w przemyśle lotniczym i samochodowym. Jednakże ze względu na strukturę heksagonalną zwartą, skutkującą niewystarczającą liczbą systemów poślizgu, stopy magnezu wykazują złą plastyczność w temperaturze pokojowej. Konwencjonalne metody umocnienia poprzez zgniot wymagają temperatury około 300°C dla tych stopów, co sprzyja jednocześnie procesom zdrowienia i rozrostu ziarna, ale obniża sam efekt umocnienia. Zatem kluczowe jest rozwinięcie technologii dla półproduktów ze stopu magnezu, która zapewni lepsze właściwości mechaniczne końcowych produktów poprzez uformowanie korzystnej mikrostruktury. W pracy przedstawiono rozwój tekstury krystalograficznej stopu na bazie magnezu (Mg-AZ31) w formie rury wyciśniętej w temperaturze 430°C i poddanej walcowaniu pielgrzymowemu we względnie niskiej temperaturze.

1. Introduction

In spite of relatively high specific strength, practical applications of magnesium and its alloys are restricted by their insufficient plasticity at room temperature – the typical disadvantage of metals with the hexagonal close-packed (*hcp*) lattice. The limited plasticity results from insufficient number of the independent systems of easy slip (two systems instead of five ones required for general strain accommodation). Two main slip systems belong to the basal plane of the hexagonal lattice and are called the basal-slip systems. Deficiency of slip systems is partially compensated by the mechanical twinning, which strongly depends on deformation mode: tension or compression, related in turn to the orientation of particular grain. Thus, a specific crystallographic texture of the sample may lead to extensive mechanical twinning, enhancing ductility at desired range of ambient temperatures. Furthermore, the twinning can noticeably strengthen or weaken the material depending on specific circumstances [1-3].

In order to improve the plasticity, conventional methods of plastic forming are usually performed at the elevated temperatures (e.g. the typical homological temperature of extrusion is above 0.6) so that the non-basal slip systems can be then easily activated, increasing the ductility of the Mg-based alloys. According to *Doege et al* [4] non-basal slip can be activated at temperatures above 225°C. Unfortunately, high-temperature processing results in the loss of beneficial effects of deformation strengthening, which is especially important in the case of products meeting high requirements, such as pipes.

In this study, the possibility of applying the pilger rolling to strengthen the hot-extruded pipes from the *Mg-AZ31* alloy was tested. It was expected that a precise control of the rolling parameters (deformation and temperature) would not only improve the mechanical properties of the hot-extruded products but also increase their quality (reduce the surface roughness). The paper is focused on characterization of the crystallographic texture (both the global and the local one) and the microstructure development (the grain size, its shape and

* INSTITUTE OF METALLURGY AND MATERIALS SCIENCE PAS, 25 REYMONTA STR., 30-307 KRAKÓW, POLAND

** AGH UNIVERSITY OF SCIENCE AND TECHNOLOGY, AL. A. MICKIEWICZA 30., KRAKÓW, POLAND

*** FOUNDRY RESEARCH INSTITUTE, 73 ZAKOPIAŃSKA STR., KRAKÓW, POLAND

Corresponding author: p.drzymala@imim.pl

disorientation distribution - see Appendix) during the applied deformation mode. Formation of texture and grain refinement in the context of material's hardness was also analyzed. Moreover, relations between slip and mechanical twinning mechanisms acting during the pilger rolling process were investigated. Such relations can be helpful in the development of technology of high quality tubes made from Mg-based alloys.

2. Experimental

The experiments were carried out on a pipe made of a commercially available magnesium alloy Mg + 3%Al + 1%Zn + 0.2%Mn (*Mg-AZ31*). The pipe (diameter 20 mm, wall thickness 4.5 mm) was produced by NeoCast - Light Metal Technologies Company [5] in a hot-extrusion process at 430°C with the extrusion ratio equal to 9. We will refer to this material as the initial one. Then the pipe was pilger rolled with mandrel at temperatures significantly lower than 300°C. The deformation gradually increased during the rolling: for each tested deformation temperature a critical deformation level (*CDL*) was observed, above which the material begins to crack and crumble. The material examined in the present paper was deformed with *CDL* close to 55% reduction of the pipe wall thickness at the temperature of 200°C. Investigated samples exhibit deformation from initial state 0% to 5%, 13%, 28% and 50% reduction of the pipe-wall thickness. The results of microstructure examination (optical- and scanning electron microscopy), texture analysis (X-ray and the electron backscatter diffraction techniques), and microhardness measurements were collected on the samples' surfaces marked in Fig. 1.
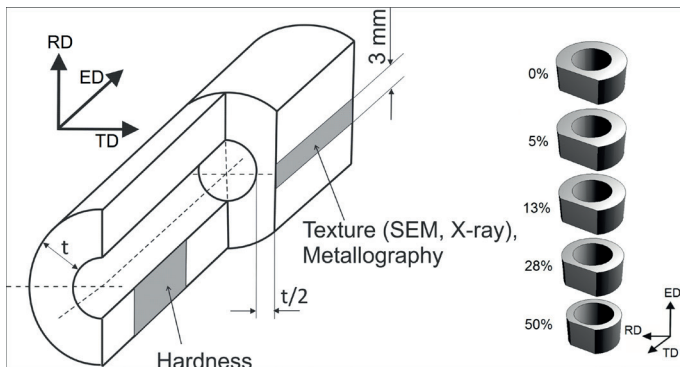

Fig. 1. Scheme of the examined samples' cross sections and list of pipes selected for investigation. The adopted reference coordinate system: *ED* - elongation direction, *TD* - tangential direction and *RD* - radial direction

The examined surfaces of the samples were prepared by polishing with the SiC polishing paper (up to the final grit equal to 4000) and then with diamond paste (particle diameters of 6.0, 3.0, 1.0 and finally 0.25 μm). The samples for microscopic studies were etched in the solution of acetic acid (10 ml), water (10 ml) and 4% solution of picric acid in ethanol (70 ml).

Metallographic and micro-hardness analyses were performed on longitudinal cross-sections of the pipe (Fig. 1) with the use of optical microscope *Carl Zeiss Jena Neophot 32* and the *Tukon 2500* (by *Wilson*) hardness tester. The

microhardness measurements were performed using the Knoop's indenter with 0.1 kg load, in compliance with the ISO 4545. Two series of measurements were performed, covering whole range of the pipe wall thicknesses. In one series, the longer diagonal of indenter was parallel to the elongation direction (*ED*), in the other one it was parallel to the radial direction (*RD*).

The global crystallographic textures were characterized by the orientation distribution functions (*ODFs*). Complete and inverse pole figures were calculated from the incomplete pole figures with the *LaboTex* software package [6] based on the arbitrary defined cells (*ADC*) method [7,8]. The incomplete pole figures of (0001), (10$\bar{1}$0), (10$\bar{1}$1), (10$\bar{1}$2) and (10$\bar{1}$2) -lattice planes were mesured with the X-ray texture goniometer Bruker *D8-Discover*. The back-reflection Schultz method [9] with *CoKα*-series radiation was used. The measurement was performed on the longitudinal cross sections in the middle of pipe-wall thickness (Fig. 1). The applied *X-ray* incident beam was shaped by a polycapillary optics and a pinhole collimator. This allowed restricting the measurement area to ca. 2.0 mm², located precisely in the intended point on the examined surface of the sample. An equiangular measurement grid [10], in range of polar angle $\alpha \in [0 \div 75°]$ and azimuthal one $\beta \in [0 \div 360°]$ with the step $\Delta\alpha = \Delta\beta = 5°$, was applied. For this work a specialized methodology of measurements was applied. At each measurement point of a pole figure (α, β) a defined angular part ($\Delta 2\theta$) of diffraction spectra was recorded and deconvolution procedure was applied to extract precisely the integrated intensity of single diffraction peak. Such procedure was necessary because of the relatively small differences in Bragg angle for the strongest Mg reflections, which in presence of residual stress existing in deformed material result in partial overlapping of observed diffraction lines. Earlier, the same procedure was successfully applied for the quantitative phase analyses of textured materials [11].

The electron backscatter diffraction (*EBSD*) *measurements were carried out* with the scanning electron microscope *FEI-Quanta 3D FEG equipped with TexSEM Laboratories EBSD system.* Analysis of the *EBSD* results was performed using a dedicated software developed at IMMS PAS that allows elaborated correcting and filtering orientation maps and reveals accurate characteristics of disorientations between the grains [12, 13].

3. Results and discussion

The hardness measurements confirmed that investigated processing of Mg-AZ31 alloy strengthen the material. The micro-hardness test performed at two arrangements of the Knoop indenter longer axis, i.e. parallel to ED and parallel to RD, revealed anisotropy of mechanical properties of the examined pipe (Fig. 2). The Knoop's hardness (HK) values were significantly higher for RD orientation of the longer axis of intender in comparison to the ED orientation of longer intender's axis. For RD intender orientation average values of the HK were 66.4, 70.8, 86.5, 90.5, and 91.7 for deformations 0%, 5%, 13%, 28% and 50%, respectively. In case of ED intender orientation average values of HK were 53.4, 57.8, 78.5, 68.4, 71.4 for the same deformations sequence Thus, due to applied

deformation at least 33% increase in hardness was observed. The respective HK ratio for the both intender orientations was 1.25 (±0.032), 1.22 (±0.039), 1.10 (±0.020), 1.31 (±0.029), 1.28 (±0.056). The observed changes in anisotropy can be induced by transformations of crystallographic texture during the applied deformation in pilger rolling process.
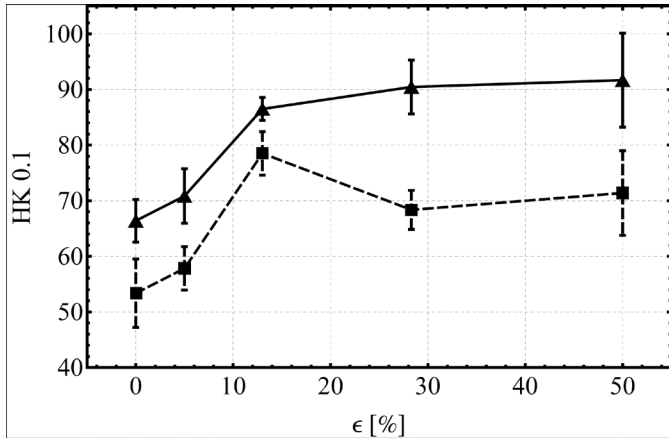

Fig. 2. Results of microhardness test for sample deformed up to c.a. 50% with RD (solid line) and ED (dashed line) arrangement of the longer edge of Knoop's intender. Error bars are standard deviations for series of measurements

The microstructure of the initial state of the investigated material (Fig. 3) was characterized by the presence of coarse grains (size of 10-80 μm) surrounded by small nearly equiaxed grains. The equiaxed grains (size up to 5 μm) formed irregular clusters at the boundaries of larger, often elongated ones. Such microstructure was formed during the dynamic recrystallization of extruded material. The determined area-weighted average grain size equal to 15.8 μm is close to the value found by Chiang at al. [14] in the extruded Mg-AZ31 alloy and significantly exceeds grain size present in commercial sheets [15] and rods extruded at 300-450°C, where it is in the proximity of 10 μm [16].

The presence of twins in some grains in the Mg-based alloy extruded at 430°C has been already reported in the literature [17–19]. However, *Chiang at al.* [14] found no evidence of twinning in the microstructure of the alloy after hot extrusion at 400°C. The role of grain orientation in the process of mechanical twinning is well known and explained by the polarization effect of the twin shear [20]. It can be said that observations of various regularities in microstructure morphology, registered in the current study, suggests hypothetical effect similar to twin shear polarization and occurring in the dynamically recrystallized Mg-based alloys, which is interesting field for further investigation.

The microstructure inhomogeneity, like group of several adjacent grains cut by the shear bands, is typical for the deformed material (see Fig. 3). Deformation process significantly refines the grains. The area-weighted average grain size of the sample deformed to 13% is ca. 8.3 μm. We observed that the deformation close to the *CDL* (in the examined alloy *ca.* 55%) can lead to microstructure with grain size below 2 μm, containing considerable amount of twins.
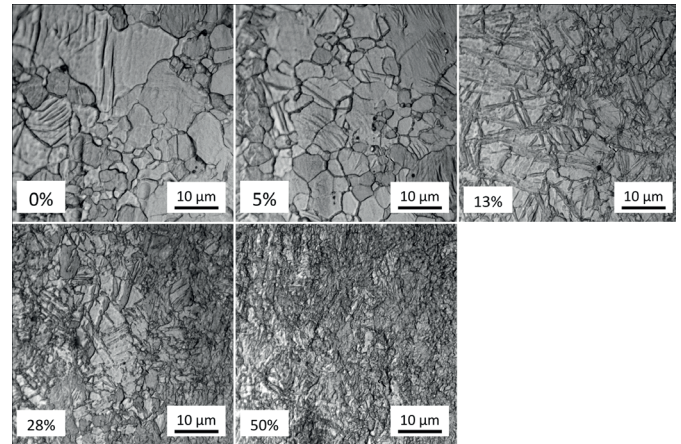

Fig. 3. Microstructure of the Mg-AZ31 pipe wall (side-section) after hot extrusion; initial state (0%) deformation up to 50%. The scale bars (the same for each picture) denotes distance 10 mm

The texture evolution manifested by a spatial orientation of basal (0001), prismatic $(10\bar{1}0)$ and pyramidal $(10\bar{1}1)$-lattice planes is shown in Tab. 1 and Fig. 4. The material exhibited a very strong crystallographic texture already in the initial state (directly after extrusion). A spread fibre $< 10\bar{1}0 >$ component which manifests by arrangement of $\{10\bar{1}0\}$-planes perpendicular to ED and $\{0001\}$-planes parallel to this direction dominates in texture of the pipe-wall. Additionally, the $\{0001\}$-planes are rotated to some extent (left- and right hand) around ED with respect to position of the maximal intensity of (0001)-pole figures which corresponds to the tangential direction a perpendicular both to the radius and length of the pipe. The amplitude of this rotation achieves 90° and is manifested as $\{0001\} \div \{11\bar{2}4\} < \bar{1}100 >$ orientations strongly spread around ED towards RD. The texture is similar to the typical fibre texture of extruded AZ31-alloy for which the basal plane is parallel to the extrusion direction [3,16]. Initial extent of the orientation spread keeps up to *ca.* 13% reduction of the pipe wall thickness and then diminishes distinctly. A more detailed texture analysis based on the ODF function allowed to identify transformation of crystallographic texture during material deformation and twinning.
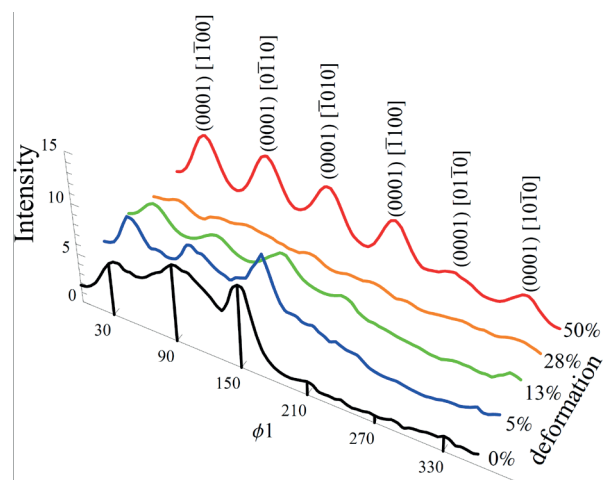

Fig. 4. Integrated skeleton lines (intensity vs. φ_1 angle) of the orientation distribution function represented in the Euler space (φ_1, Φ, φ_2) for the initial (deformation 0%) and deformed (5%, 13%, 28% and 50%) states of the investigated material

Recalculated pole figures of selected crystallographic lattice planes vs. deformation degree for Mg-AZ31 samples of extruded pipe: initial state with 0% of deformation and after pilger rolling with deformation 5%, 13%, 28% and 50%
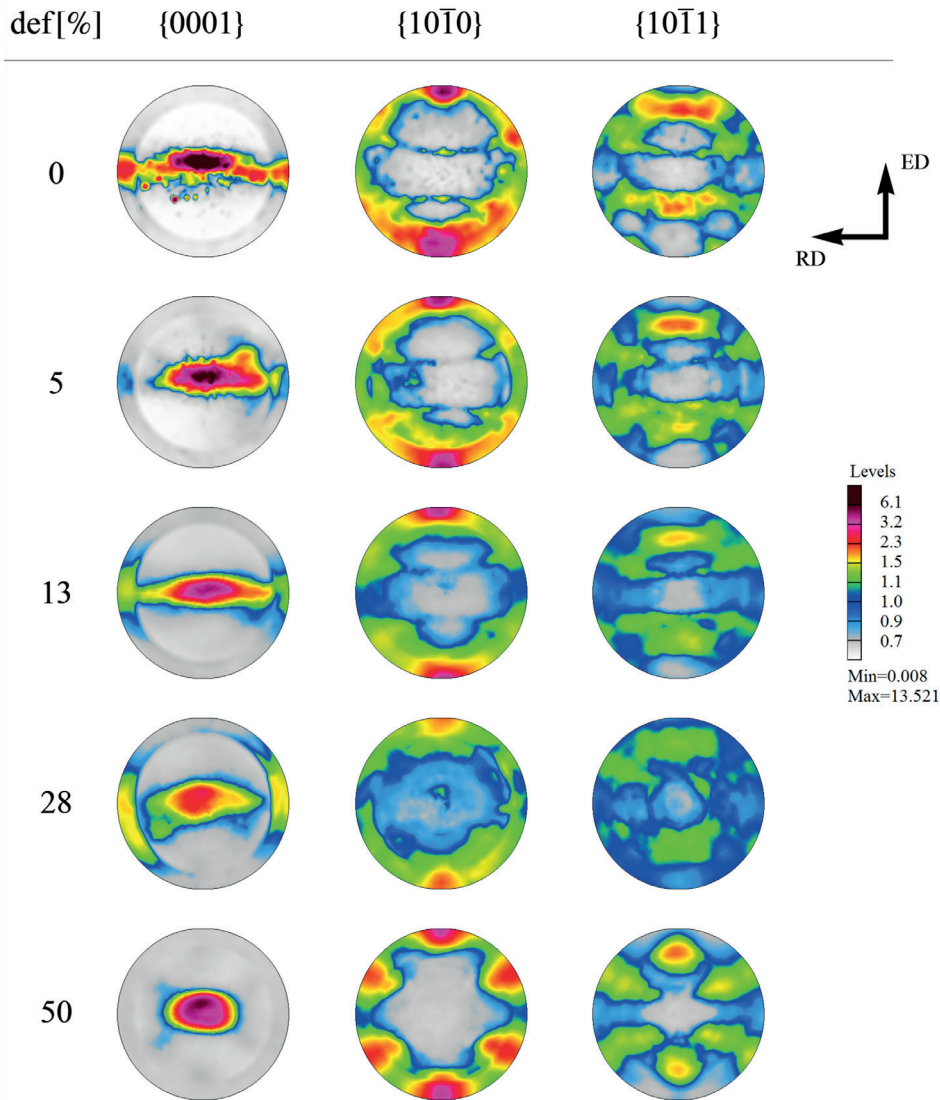
The ODF is a function described in orientation space consisting of three independent variables, the Euler angles φ_1, Φ, φ_2, and the skeleton line is defined as a function of one selected independent variable – here the φ_1 [21] – connecting the local maxima of the ODF (integrated over $\Delta\varphi_1 = 10^0$, $\Delta\Phi = 10^0$, $\Delta\varphi_2 = 10^0$ voxel). Skeleton lines depicting the main texture components for initial and deformed material are given in Fig. 4. Because of strong basal fibre texture, the skeleton lines describe six $\{0001\}< 10\bar{1}0 >$ type of maxima, which are located in vicinity of $\Phi = 0^0$, $\varphi_2 = 0^0$ for the whole range of φ_1. Thus the skeleton lines values come from integration of the ODF over the $[0, 10^0]$ range for Φ and φ_2 and are presented in function of φ_1. One can see that the dominant $(0001)[1\bar{1}00]$, $(0001)[0\bar{1}10]$ and $(0001)[1010]$ maxima of the initial material texture decreased successively with increased deformation up to 28%. However, further increase of deformation (up to 50%) caused increase of the maxima intensities when compared to the initial level. Moreover, with increasing deformation the texture becomes more and more symmetric in respect to TD (see Tab. 1).

Both microstructure and local crystallographic texture calculated from a set of single orientations measured with the orientation imaging microscopy (OIM - SEM/EBSD) (Fig. 5) confirmed that the grain size distribution is closer to the hyperbolic than to the lognormal distribution, with the average area-weighted grain size ca. 16 μm in the initial material state. A similar type of the distribution was observed for the deformed alloy, but in that case grain size systematically decreased with deformation (see Fig. 3).

Two types of single twins (tension- $\{10\bar{1}2\} < 10\bar{1}1 >$ and contraction twin $\{1011\} < 10\bar{1}2 >$), double contraction-tension twins (DTW) $\{10\bar{1}1\} - \{10\bar{1}2\}$ and extension-extension twins (ETW-ETW) $\{10\bar{1}2\} - \{10\bar{1}2\}$ were identified by OIM (Fig. 5). The same types of twins were previously reported by *Ando et al*. [22] and *Mu et al*. [23]. The disorientation related to the $\{10\bar{1}2\} < 10\bar{1}1 >$ and $\{1011\} < 10\bar{1}2 >$ twinning is equal to 86.3° and 56.2° [22-25], respectively. For double twins: $\{10\bar{1}1\} - \{10\bar{1}2\}$ DTW

and $\{10\bar{1}2\} - \{10\bar{1}2\}$ ETW-ETW the disorientation angles are 37.5°, 69.8°, 66.5°, 30.2° and 7.3°, 60.4°, 60.0°, respectively [22, 23]. Intensity of the particular twinning can be tracked by analyzing the changes in the disorientation distribution (Fig. 6 and 7). For identification of twin boundaries we assumed 5° deviation of angle and axis from the ideal disorientation values.

For analysis of twinning with the use of EBSD orientation maps, the obtained data was divided into consistent sets of similar orientations representing the individual grains. The sets were characterized by their average orientation, area fraction and parameters of disorientation with the neighbouring grains. In the initial material the $\{10\bar{1}2\} < 10\bar{1}1 >$ tension twins were most common and other types of twins were relatively rare, but their presence increased significantly with deformation up to 13%. Similarly, the global X-ray textures indicated that $\{10\bar{1}2\} < 10\bar{1}1 >$ twinning contributes to the components observed in the final texture. Texture anisotropy was defined as the ratio of the $\{0001\} < 2\bar{1}\bar{1}0 >$ and $\{0001\} < 1\bar{1}00 >$ orientations. The ratio determined on OIM results was equal to 0.74 for initial material and 0.83 for 13%-deformed (Fig. 5) and corresponded to data obtained from X-ray measurements: 0.75, 0.74, 0.79, 0.90, 0.61 for 0%, 5%, 13%, 28% and 50% deformation, respectively (Table 1 and Fig. 4). This confirms that the analyzed OIM data sets can be considered as representative for the investigated material.

Fig. 6. Histogram of disorientation angles for initial (solid) and 13%-deformed (dashed) sample

Fig. 7. Histogram of disorientation angles related with rotation of two neighbouring crystallites around <1000> axis (tolerance angle 5°) for initial- (solid) and 13%-deformed (dashed) sample
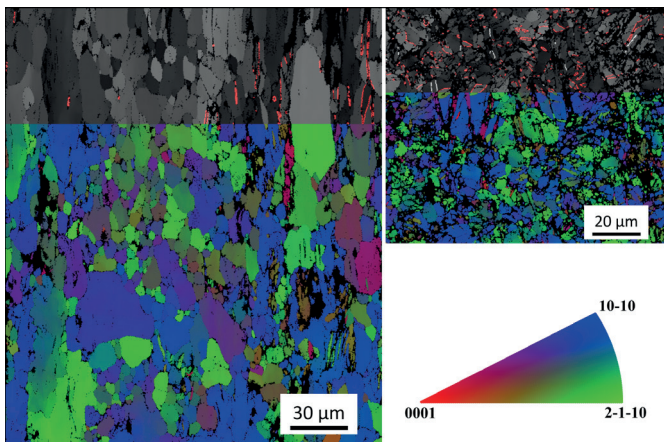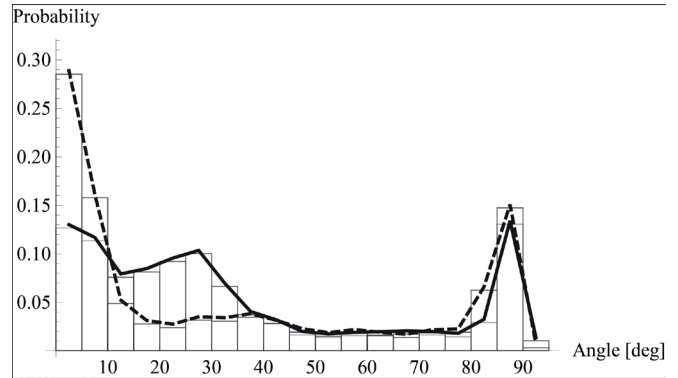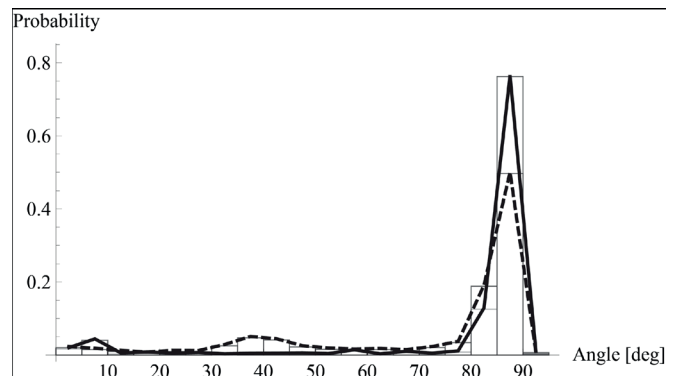

Fig. 5. OIM filtered by orientation coherency of the initial alloy state (left) and 13% cold worked deformation of material (right). Identified grains coloured with the stereographic projection of ED direction in the standard stereographic triangle for hexagonal crystals. Amount of map points with orientation successfully determined: 88% and 68%, respectively. On the gray-shadowed parts of the orientation maps the twin boundaries are presented in red colour and DTW variant with 37.5° disorientation angle is shown in white colour

In Fig. 6, three maxima of disorientation angles (0°, 27° and 86°) for the initial sample and two maxima of disorientation angles (0° and 86°) of 13% deformed sample can be distinguished. The low angle maximum can be ascribed to grain fragmentation, as its value increased rapidly in deformed sample. Disappearance of the 27° local maximum is related with its relative decreasing presence in the boundaries population, due to fragmentation of grains building maximum for small angles. The 86° maximum indicates tensile twinning.

A more detailed description of grains disorientations can be performed in Rodrigues space (see Appendix). The specified grain disorientations (twins) were characterized, apart from angle values, by their position in the asymmetric domain for the *hcp* crystal lattice (Fig. 8 and 9). Such procedure allowed to distinguish specified disorientations and randomly oriented pairs of grains with the same disorientation angles. Fig. 7 depicts histogram of disorientations related with rotation around $< 2\bar{1}\bar{1}0 >$ axis for initial and 13%-deformed material. The disorientation angle of ca. 86° dominates in microstructure of these materials. It means that the tensile twinning by $\{10\bar{1}2\}$ planes was the most frequent grain to grain relation in investigated alloy up to 13% of deformation of extruded pipe. Relative high local maxima for 38° rotation angle (Fig. 7) belongs to the $\{10\bar{1}1\} - \{10\bar{1}2\}$ DTW variants for 13% deformed sample. The local maximum around 27° in the histogram of disorientations for initial sample (Fig. 6, solid line) can be ascribed to disorientations with random axis in Rodrigues disorientation space depicted in Fig. 8.
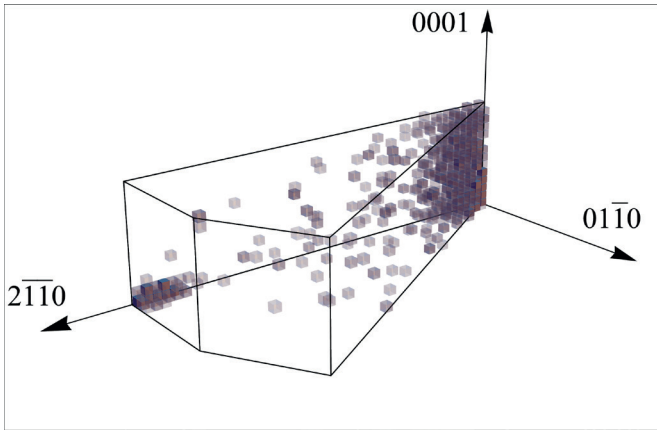
Fig. 8. Disorientation distribution of the extruded state of the investigated Mg-AZ31 alloy. Axes labels denote crystal directions
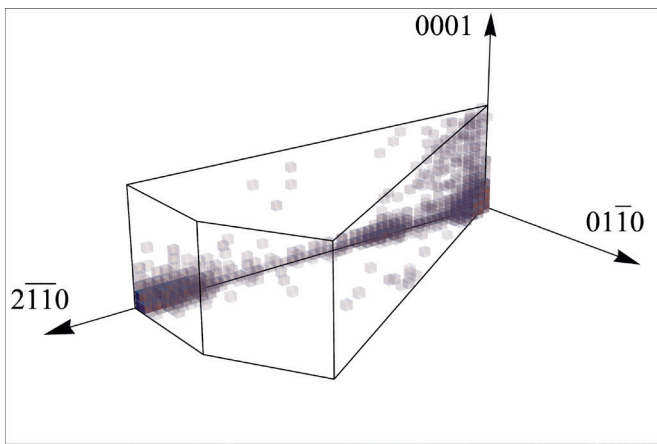

Fig. 9. Disorientation distribution of the 13% deformed state of the investigated Mg-AZ31 alloy. Axes labels denote crystal directions

A significant difference between the specific disorientation distribution for the initial- and deformed (13%) state of the material lies in intensity of the twinning disorientation angle component. Thus, the distribution given in Fig. 9 reveals that this type of twinning was dominant deformation mechanism in pilger rolling process. We observed increase of twin boundaries in respect to the total length of grain boundaries. The fraction of grain boundaries for tension twinning increased from 0.14 to 0.18. Simultaneously the identified twin boundaries (any type of twinning) increased from 0.16 to 0.24.

4. Conclusions

1. It was found that at least 33% increase in hardness can be obtained due to the pilger rolling of hot extruded Mg-AZ31 pipes. For this purpose only 13% deformation was sufficient. The hardening was due to change in microstructure i.e. refining of the grain size from 15.8 to 8.3 μm, change in the crystallographic texture and substantial increase in the twins density.
2. The {0001} type of texture remains unchanged, which is clearly visible on the pole figures, but the intensity of {0001}-poles is a function of deformation. Up to 28% of deformation, weakening of texture occurs and can be easily observed on the ODF skeleton line located in

10^0 vicinity of $\Phi = 0^0$ and $\varphi_2 = 0^0$ and the whole range $[0,360^0]$ of φ_1. During the pilger rolling process the ratio of weaker texture maximum $\{0001\} < 2\bar{1}\bar{1}0 >$ to dominant fibre maximum $\{0001\} < 1\bar{1}00 >$ (anisotropy) of the initial texture increased up to 28% reduction of the tube thickness. The ratio of these two components can be treated as a measure of wire texture randomisation. The initial material's strong anisotropy of texture was described by the ratio 0.75. Pilger rolling increased this ratio to highest value 0.90 (small anisotropy) at 28% of deformation, but then lessened it to 0.61 (very strong anisotropy) at 50% of deformation just before crack.

3. The microstructure of hot extruded pipe consisted of coarse and elongated grain and a number of small equiaxed grains resulting from dynamic recrystallization. Pilger rolling resulted in twinning and fragmentation of coarse grains. The identified twins were mostly $\{10\bar{1}2\} < 10\bar{1}1 >$ tension twins and also $\{10\bar{1}1\} - \{10\bar{1}2\}$ DTW. About 50% increase of the twin grain boundaries resulted from 13% of the deformation, in which only the increase in the tension twin boundaries was ca. 30%.

4. Due to changes in texture, pilger rolling process decreases hardness anisotropy of the pipe wall expressed as the ratio of hardness measured in parallel and perpendicular direction (from 1.25 to 1.10 up to 13% of deformation). However, higher degrees of deformation increased the anisotropy to value exceeding the initial state. The drop in anisotropy value at 13% deformation can be related to weakening of the initial texture. On the other hand the sample deformed to 28% with the weakest texture had the maximum value of hardness anisotropy. The increase in the anisotropy observed for the deformation range 13-28% can result from the change in the type of texture.

5. Appendix

Misorientation denotes any transformation from one crystal reference frame to crystal one, while disorientation is defined as the misorientation with the smallest rotation angle in the selected asymmetric domain. For the given two orientations ascribed to microstructure area located near the identified grain boundary the set of all possible (12 x 12 x 2) misorientations were calculated in terms of rotation matrix operators. The formula consisted of 12 symmetrically equivalent rotation matrices of the first orientation multiplied by same amount of inversed rotation matrices for the second orientation. Inverse order of the orientations (from the second to the first) was also included in the calculation procedure (switching symmetry) and the resulting misorientations were parameterized in Rodrigues-Frank (R-F) vectors. By definition only one of the disorientation is represented in the RF asymmetric domain [26].

The calculated RF vectors for tension and compression twins are respectively (0.9376, 0, 0) and (0.5333, 0, 0). For $\{10\bar{1}1\} - \{10\bar{1}2\}$ DTW relation, possible RF vectors are; (0.3399, 0, 0), (0.6799, 0, 0.1587), (0.6251, 0.050, 0.1925),

(0.2696, 0, 0) and for $\{10\bar{1}2\} - \{10\bar{1}2\}$ ETW-ETW the variants of RF vectors are; (0.0645, 0, 0), (0.5333, 0.2334, 0) and (0.4990, 0.2881, 0.0371).

REFERENCES

[1] M.H. Yoo, Slip, twinning, and fracture in hexagonal close-packed metals, Metall. Trans. A **A12**, 409-418 (1981).

[2] M.R. Barnett, Twinning and the ductility of magnesium alloys, Part I: Tension twins, Mater. Sci. Eng. A **464**, 1-7 (2007).

[3] S.A. Agnew, Ö. Duygulu, Plastic anisotropy and the role of non-basal slip in magnesium alloy AZ31B, Int. J. Plast. **21**, 1161-1193 (2005).

[4] E. Doege, W. Sebastian, K. Droder, G. Kurz, Increased formability of Mg-sheets using temperature controlled deep drawing tools in innovations in processing and manufacturing of sheet materials, TNS Annual Meeting, 53-60 (2001).

[5] http://www.en.neocast.pl.

[6] K. Pawlik, P. Ozga, LaboTex: The texture analysis software, Göttinger Arbeiten zur Geologie und Paläontologie, SB4 (1999).

[7] K. Pawlik, Determination of the orientation distribution function from pole figures in Arbitrarily Defined Cells, Phys. Status Solidi B **134**, 477-483 (1986).

[8] K. Pawlik, J. Pospiech, A method for the ODF approximation in Arbitrarily Defined Cells from pole figures, in: Bunge HJ (ed) Theoretical methods of texture analysis. DGM Informationsgesellschaft Verlag, Oberursel (1987).

[9] L.G. Schulz, A direct method of determining preferred orientation of a flat reflection sample using a geiger counter X-ray spectrometer, J. Apply Phys. **20**, 1030-1033 (1949).

[10] L. Tarkowski, L. Laskosz, J. Bonarski, Optimisation of X-ray pole figure measurement, Eighth European Powder Diffraction Conference, May 23-26, 2002 Uppsala, Sweden: Mater. Sci. Forum **443-444**, 137-140 (2004).

[11] J.T. Bonarski, M. Wróbel, K. Pawlik, Quantitative phase analysis of duplex stainless steel using incomplete pole figures, Mater. Sci. Technol. **16,** 6, 657-662 (2000).

[12] K. Sztwiertnia, J. Kawałko, M. Bieda, K. Berent, Microstructure of polycrystalline zinc subjected to plastic deformation by complex loading, Arch. Metall. Mater. **58**,1, (2013).

[13] A.G. Checa, J.T. Bonarski, M.G. Willinger, M. Faryna, K. Berent, B. Kania et al. Crystallographic orientation inhomogeneity and crystal splitting in biogenic calcite, J. R. Soc. Interface **10**, 86, 04-25 (2013).

[14] L. F. Chiang, H. Hosokawa, J.Y. Wang et al. investigation on dynamic friction properties of extruded AZ31 magnesium alloy using ring upsetting method, Mater. Trans**. 51,** 7, 1249-1254 (2010).

[15] H. Koh, T. Sakai, H. Utsunomiya, S. Minamiguchi, Deformation and texture evolution during high-speed rolling of AZ31 magnesium sheets, Mater. Trans. **48,** 8, 2023-2027 (2007).

[16] K.P. Rao, Y. V. R. K. Prasad, J. Dzwonczyk, N. Hort, K.U. Kainer, Hot deformation mechanisms in AZ31 magnesium alloy extruded at different temperatures: Impact of Texture, Metals **2**, 293-312 (2012).

[17] M. Huppmann, M. Lentz, S. Chedid, W. Reimers, Analyses of deformation twinning in the extruded magnesium alloy AZ31 after compressive and cyclic loading, J. Mater. Sci. **46**, 938-950 (2010).

[18] M. Huppmann, M. Lentz, K. Brömmelhoff, W. Reimers, Fatigue properties of the hot extruded magnesium alloy AZ31, Mater. Sci. Eng. A **527**, 5514-5521 (2010).

[19] T. Al-Samman, G. Gottstein, Dynamic recrystallization during high temperature deformation of magnesium, Mater. Sci. Eng. A **490**, 411-420 (2010).

[20] M. Wróbel, Mechanical twinning in cubic crystals, Dissertations, Monographs No 234, AGH University of Science and Technology Press, Kraków 2011-in polish.

[21] H.J. Bunge, Texture analysis in materials science, Butterworths, London (1982).

[22] D. Ando, J. Koike, Y. Sutou, Relationship between deformation twinning and surface step formation in AZ31 magnesium alloys, Acta Mater. 58, 4316-4324 (2010).

[23] S. Mu, J.J. Jonas, G. Gottstein, Variant selection of primary, secondary and tertiary twins in a deformed Mg alloy, Acta Mater. **60**, 2043-2053 (2012).

[24] M.D. Nave, M.R. Barnett, Microstructures and textures of pure magnesium deformed in plane-strain compression, Scr. Mater. **51**, 881-885 (2004).

[25] P. G. Partridge, The crystallography and deformation modes of hexagonal close-packed metals, Met. Rev. **12**, 169-191 (1967).

[26] A. Morawiec, Orientations and rotations: computations in crystallographic textures, Berlin: Springer-Verlag (2004).